2023 62nd IEEE Conference on Decision and Control (CDC)
December 13-15, 2023. Marina Bay Sands, Singapore

Multi-Occlusions Inference from Multiple Social Vehicles

Xuhe Zhao[1], Chaojie Zhang[1] and Jun Wang*[1]

Abstract— **Occlusions at intersections threaten the safety of autonomous driving, especially in urban scenarios. Phantom vehicles are usually considered to mitigate the risks associated with the occlusions, and their states may be inferred from observable vehicles. This paper extends these methods to deal with multiple occlusions and multiple inferences. A multi-occlusion aware model allows for the concerns of occluded areas and the configuration of phantom vehicles. The evidence theory fuses multiple estimations to enhance occlusion inferences. Simulations for intersection scenarios are conducted to demonstrate the effectiveness of the proposed method for improving traffic efficiency.**

I. Introduction

Significant progress has been achieved in autonomous vehicle planning in recent decades. However, challenges persist due to uncertainties of driving scenarios, sensor range limitations, and complex interactions with human drivers. In some urban traffic scenarios, there are usually multiple dynamic and static occlusion factors (such as buildings, vehicles, etc.), and the ego vehicle cannot directly perceive the positions and speeds of potential traffic participants in the occluded areas. As shown in Fig. 1, when the ego vehicle is about to turn left at an intersection, there are obstructions such as parked cars and buildings around, blocking the view of the ego vehicle. The dynamic vehicles in the occluded areas may threaten the driving safety.

To deal with the uncertainty caused by occlusions, it is necessary to establish an appropriate model to describe the traffic situation in occluded area reasonably. A common approach is to allocate phantom vehicles at the boundaries of occluded areas, considering the worst-case. The study in [1] considered the uncertainty of intentions of phantom vehicles turning or going straight at intersections and searched for the optimal longitudinal acceleration of the ego vehicle. In [2], the configuration of phantom vehicles was refined based on traffic rules and verified in various traffic scenarios. References [3], [4] used the Partially Observable Markov Decision Process (POMDP) to model the uncertainty caused by occlusions at intersections, and described the distribution of potential vehicles as a Poisson process using traffic flow information. In addition to directly configuring phantom vehicles, particle simulations can be used to describe the potential positions of vehicles in occluded areas. The work in [5] used a particle filter to generate a probability distribution of blind spot risks and optimize safe trajectories. Reference [6] proposed a set-based model of occlusion factors, which established a unified framework for potential traffic participants. However, such overapproximation approaches may lead to conservative planning trajectories.

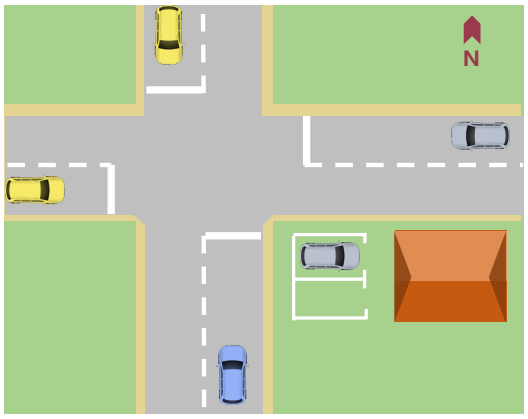

Fig. 1: The parked vehicle and buildings are occluded factors. The ego vehicle (blue) can infer occlusions based on two observed vehicles (yellow).

In urban traffic scenarios with occlusions, behaviors of observable traffic participants may contain traffic information of occlusions. Therefore, some studies inferred the traffic situation in occluded areas by analyzing the observable behaviors of surrounding vehicles [7]. The work in [8] proposed a method for inferring the occupancy probability of grid map based on human behaviors, learning the mapping from different actions of human-driving vehicles to grid occupancy probabilities. Reference [9] presented a learning-based method of multimodal mapping from observable trajectories of other vehicles to occupancy grids, and verified it in multi-vehicle scenarios. Reference [10] used inverse planning to generate the reward function of inverse reinforcement learning for inferring occlusions. Reference [11] estimated the probability distribution of occlusion configurations and intentions of other vehicles by inverse planning. Various methods have been proposed for occlusion inference by using observable traffic participants as sensors, but these methods are only applicable to single-occlusion scenarios. Reference [9] provided a solution to dealing with multiple sensor measurements. It fused the grid occupancy probabilities of the front view of each observed vehicle with the evidence theory. However, end-to-end inference methods based on occupancy grid map have difficulty in fusing traffic rules and cannot explicitly describe the types of traffic participants.

Inspired by [6] and [9], this paper proposes an occlusion inference framework suitable for urban scenarios using social

[1]Xuhe Zhao, Chaojie Zhang and Jun Wang are with the Department of Control Science and Engineering, Tongji University, Shanghai 201804, P. R. China.
[2]*Corresponding author, e-mail: junwang@tongji.edu.cn.

vehicles as sensors. The main contributions of this paper are as follows:

- The proposed model is applicable to multiple occlusions.
- The inference incorporates occluded area estimations from multiple social vehicles.
- The occlusion inference is applied to improve traffic efficiency.

The remaining sections are organized as follows: Section II describes the multi-occlusion modeling method in detail. Section III presents the process of multi-sensor inference and integrates the inference into a POMDP module. Section IV carries out simulations and the corresponding analyses. Section V summarizes and outlooks the proposed method.

II. Multi-Occlusion Aware Model

Urban traffic scenarios usually involve multiple occlusions. This paper proposes a multi-occlusion aware model, which filters occluded areas of interest and reasonably configures phantom vehicles in urban scenarios.

A. Environment Model

In this paper, the environment model updated at each time step consists of the following elements.

1) FOV: The FOV is given by the upstream perception module, and is related to the position and height of the occlusion and the perception performance. This paper ignores sensor noise and analyzes the occlusion areas centered on the ego vehicle from a bird's eye view.

2) Traffic Participants: All traffic participants in the environment at t are noted as $p_t \in P_t$, $p_t := \langle c^p, s_t^p, Q^p \rangle$. In driving scenarios with occlusions, the vehicles can be divided into three categories, i.e. observed traffic participants, phantom traffic participants and the ego vehicle. The type is denoted by $c^p \in \{'\mathrm{ob}','\mathrm{pht}','\mathrm{ego}'\}$. The state $s_t^p := [x_t, y_t, v_t, \phi_t]^T$ contains the position, speed and yaw of the traffic participant. And Q^p is the parameters of each traffic participant. In this paper, vehicles are considered as the only type of traffic participants for simplicity, and other participants such as bicycles and pedestrians can be modeled similarly.

3) Road Topology: The road topology is based on lanelet maps [12]. A road topology node consists of one lanelet cell or multiple laterally adjacent lanelets. Each road topology edge indicates the adjacency of nodes. The lanes in connected nodes are longitudinally adjacent, and the direction of the edge is the same as lanes. Each node represents a segment of the lane physically, and there may exist overlapping areas between different nodes. A road topology layer is illustrated in Fig. 2(a).

B. Phantom Vehicle Model

This paper proposes a phantom vehicle model, which provides a unified and explicit representation of potential vehicles.

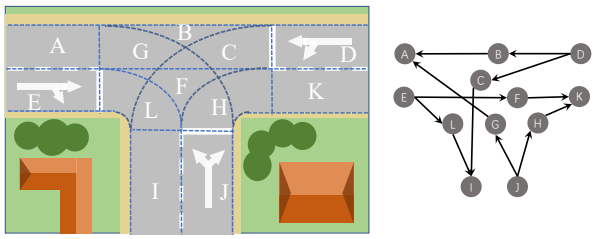

(a) Road network of T-intersection.

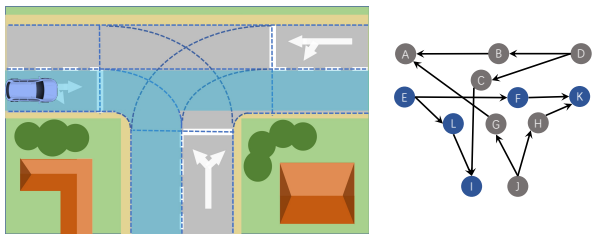

(b) Intention of the blue vehicle is unknown.

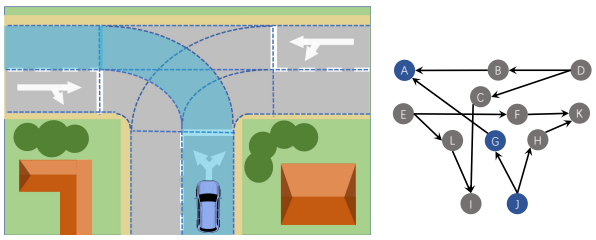

(c) Intention of the blue vehicle is turning left.

Fig. 2: Road topology.

1) Positions of Phantom Vehicles: The driving corridor is a sequence of lanes which a vehicle is likely to travel through. The breadth-first search is performed on the road topology layer for each vehicle to obtain its driving corridor. The parameter $b_{dir} \in \{'\mathrm{drivDir}','\mathrm{anyDir}'\}$ indicates the constraint of the driving intention of the vehicle during the search, as shown in Fig. 2(b) and Fig. 2(c). If the driving corridors of two vehicles intersect, they are at risk of potential conflict, and the intersecting part is called the conflict area.

The occluded areas at current time can be obtained according to the environment model Ω. The intersection points of all lane midlines with the boundary of the occluded areas, $\zeta_t^k := \left(x_t^k, y_t^k\right)$, indicate the possible location of the kth phantom vehicle. Configure the candidate phantom vehicles at each ζ_t^k, and check for potential conflicts between the driving corridors of the ego vehicle and the candidate. The candidates impossible to conflict with the ego vehicle will be discarded. Since the model is updated in real time, among all the candidates in the same lane and traveling in the same direction, retain the one with the closest conflict area to the ego vehicle. Then the set of locations of phantom vehicles can be determined.

2) Speeds of Phantom Vehicles: This paper infers the states of potential vehicles by observing surrounding social vehicles. Therefore, we instantiate the corresponding

phantom vehicles for each observed vehicle. Essentially, the behavior of an observed vehicle is affected by the estimated time $t_{\mathrm{c}}^{\mathrm{ob,pht}}$ at which it could crash with a potential vehicle. When there are no phantom vehicles in the occluded area, or when it is impossible for potential vehicles to interact with the observed vehicle, we have

$$t_{\mathrm{c}}^{\mathrm{ob,pht}} = \infty \tag{1}$$

When the phantom vehicle is possible to interact with the observed vehicle in the future:

$$t_{\mathrm{c}}^{\mathrm{ob,pht}} = \frac{\psi_{\mathrm{c}}^{\mathrm{ob}}}{v_{\mathrm{ob}}} \tag{2}$$

where $\psi_{\mathrm{c}}^{\mathrm{ob}}$ is the distance from the location of the observed vehicle to the conflict area. Thus, for phantom vehicles with determined locations in the previous section, their speeds can be obtained by inverse extrapolation from their potential conflict time with other vehicles as follows

$$v_{\mathrm{pht}} = \min\left(\frac{\psi_{\mathrm{c}}^{\mathrm{pht}}}{t_{\mathrm{c}}^{\mathrm{ob,pht}}}, v_{\max}\right) \tag{3}$$

where $\psi_{\mathrm{c}}^{\mathrm{pht}}$ denotes the distance from the location of the phantom vehicle to the conflict point, and $v_{\max}$ is the maximum speed limit set by traffic rules.

III. Multi-Sensor Occlusion Inference

Using the behavior of social vehicles as sensors, autonomous vehicles can infer the state of potential vehicles in occluded areas. The proposed method consists of the measurement of a single vehicle sensor and fusing all measurements using the evidence theory.

A. Driver Sensor Model

Each phantom vehicle has two instantiations, i.e. the state of presence or absence. We call a possible instantiation set of all phantom vehicles an occlusion configuration, denoted by $z \in \mathcal{Z}$. The inverse-planning prediction method [13] is used to conduct the inference. The aim is to estimate the belief of each possible occlusion configuration, $\Pr(z|\hat{s}_{1:t}^{i})$, from an observed vehicle i. This paper builds a rational driver model to calculate a rational trajectory, $s_{1:\mathrm{end}}^{*i}$, for each hypothesis of observed vehicles' intention and occlusion configurations. At each planning step, the historical trajectory $\hat{s}_{1:t}^{i}$ and the predicted rational trajectory $s_{t+1:\mathrm{end}}^{*i}$ are put together as $\hat{s}_{1:\mathrm{end}}^{+i}$. Though the trajectory similarity measurement function $D(\cdot)$, defined by the longest common subsequence, we parameterize the likelihood of possible goals g and occlusion configuration z as a Boltzmann distribution with temperature β, i.e. [11]

$$L(g, z|\hat{s}_{1:t}^{i}) = \exp\left(\beta \cdot D(s_{1:\mathrm{end}}^{*i}, \hat{s}_{1:\mathrm{end}}^{+i})\right) \tag{4}$$

The prior probabilities of occlusion configurations and observed vehicle intentions are represented as $p(z)$ and $p(g)$, then the probabilistic belief of the assumptions $\Pr(z|\hat{s}_{1:t}^{i})$ can be obtained by Bayes' rule

$$\Pr(z|\hat{s}_{1:t}^{i}) \propto \sum_{g} \frac{L(g, z|\hat{s}_{1:t}^{i})p(g)}{p(z)} \tag{5}$$

B. Multi-Sensor Fusion

Urban traffic scenarios usually involve more than one observable vehicle, which provides diverse information for occlusion inference. The inference results from multiple sensors need to be fused. In this paper, the evidence theory [9] [14] is used to fuse multi-sensor information into $\mathcal{M}_{\mathrm{ego}}$. The evidence theory discriminates conflicting information (e.g., two different sensor measurements) and thus deals effectively with uncertainty inference. The hypothetical space here is $\mathcal{Z} = \{z_1, z_2, \cdots\}$, which explicitly describes phantom vehicles.

The sensor fusion process is started by heuristically transforming the probabilities in $\mathcal{M}_i$ into belief mass for occlusion measurement of the observed vehicle i:

$$m_i\left(\{z_k\}\right) = \delta\mathcal{M}_i = \delta\Pr(z|s_{1:t}^{i}) \tag{6}$$

where k is the identification of occlusion configurations. The hyperparameter δ, representing the confidence of the sensor information, is determined by the interaction between the observed vehicle and potential vehicles

$$\delta = \alpha \cdot \left(1 - \frac{N_{\mathrm{nc}}}{N_G}\right) \tag{7}$$

where $\alpha = 0.95$ is the confidence coefficient [9], N_G is the number of all possible driving corridors for the observed vehicle, and N_{nc} is the number of driving corridors without possible conflict. Thus, the uncertainty belief mass is $m_i\left(\mathcal{Z}\right) = 1 - \delta$.

At each planning step, the belief mass is updated using Dempster-Shafer's rule [14]:

$$\begin{aligned} m_{\mathrm{ego}}(z_1') &= m_{\mathrm{ego}}\left(z_1'\right) \oplus m_i\left(z_1'\right) \\ &:= \frac{\sum\limits_{z_2' \cap z_3' = z_1'} m_{\mathrm{ego}}\left(z_2'\right) m_i\left(z_3'\right)}{1 - \sum\limits_{z_2' \cap z_3' = \phi} m_{\mathrm{ego}}\left(z_2'\right) m_i\left(z_3'\right)} \end{aligned} \tag{8}$$

where $z_1', z_2', z_3' \in 2^{\mathcal{Z}}$. Initially, the ego vehicle is completely unaware of the occlusion, which means $m_{\mathrm{ego}}\left(\mathcal{Z}\right) = 1$. We can convert the belief to its probability by using Pignistic transform [15]

$$\begin{aligned} \Pr(z) &= \mathcal{M}_{\mathrm{ego}}(z) \\ &= \sum_{z' \in 2^{\mathcal{Z}}} m_{\mathrm{ego}}(z') \frac{|z \cap z'|}{|z'|} \end{aligned} \tag{9}$$

where $z \in \mathcal{Z}$, $|\cdot|$ represents the cardinality of a set.

C. Integrating Inference into Planning

The POMDP model [16] explores the optimal action sequences by constructing a search tree. The model defines the state set, action set, observation set, transition probabilities function, reward function and initial belief. It widely solves trajectory planning problems in uncertain scenarios. In this paper, the DESPOT solver in [17] is used to achieve the optimal action of the ego vehicle along a reference path.

The state space $\mathcal{S}$ and observation space $\mathcal{O}$ are set according to the model in Section II:

$$\mathcal{S} = \{s^p, g^p, z\} \tag{10}$$

where p denotes each vehicle in the scenario, $c_p \in \{'\text{ego}','\text{ob}','\text{pht}'\}$, g is the intention of each vehicle and z is the occlusion configuration.

$$\mathcal{O} = \{s^p\} \tag{11}$$

where $c_p \in \{'\text{ego}','\text{ob}'\}$.

The action space $\mathcal{A}$ consists of discrete sequences of longitude accelerations and lateral speeds.

The states of vehicles under different beliefs are transferred by the rational driver model in Section III. The initial belief b_0 is updated in real time according to the multi-sensor occlusion inference model.

The reward function includes the rewards of the the ego vehicle's speeds, accelerations and collision checks

$$\mathcal{R} = \mathcal{R}_v + \mathcal{R}_a + \mathcal{R}_c \tag{12}$$

where $\mathcal{R}_v$ considers the speed limits and path curvatures, $\mathcal{R}_a$ reflects the comfort, and $\mathcal{R}_c$ ensures the driving safety.

IV. Simulations and Evaluations

The proposed method is verified and evaluated by simulations. The simulation scenario, as shown in Fig. 1, is an unsignalized intersection where the ego vehicle will turn left from the south. A perception range of 360 degrees and 100 meters is assumed for the ego vehicle. The path of the ego vehicle is predefined based on the midline of the lane. The priority of different traffic participants is not considered in this paper.

The proposed method, named 'MultiOc Planner', was compared with two baseline planners. The aggressive planner had an optimistic estimate of the scenario, assuming that the phantom vehicles in the occluded areas would not interact with the ego vehicle. In other words, the scenario conforms to the configuration where the potential conflict time of the phantom vehicle is infinite. The conservative planner in [2] considered the worst-case scenario, assuming that all phantom vehicles in the occluded areas always exist and have potential conflicts with the ego vehicle.

Fig. 3 presents configurations of phantom vehicles and trajectories generated by the proposed planning framework. The green rectangle represents the ego vehicle, the blue vehicles can be observed, the purple vehicle is hidden behind the occlusions. The rectangle with a dotted border indicates the phantom vehicle configured for the current scenario. In the presence of multiple occlusion areas, only one phantom vehicle is configured in the position most likely to threaten vehicle safety, and collisions can still be avoided.

When there are no vehicles in the occluded area, the MultiOc planner selects a more aggressive action than the conservative planner, as shown in Fig. 4. The traveled distance of MultiOc planner is similar to that of the aggressive planner, which indicates that the proposed method can improve traffic efficiency. When there is an oncoming vehicle in the occluded area, the MultiOc planner slows down and avoid collisions, as shown in Fig. 5. In this case, MultiOc planner achieves higher passing efficiency than both baseline planners. Note that, it is caused by the aggressive

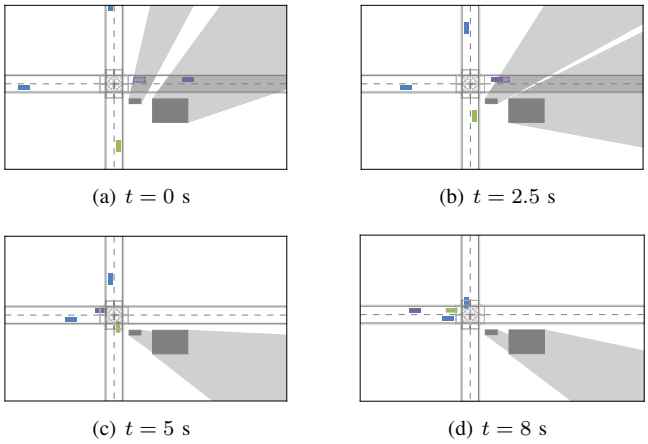

(a) $t = 0$ s (b) $t = 2.5$ s

(c) $t = 5$ s (d) $t = 8$ s

Fig. 3: Simulation results with the proposed framework.

planner's braking when an oncoming vehicle in the occluded area moves into the observable range. The average speed of trajectory generated by MultiOc planner is 12.2% higher than that of the method in [2].

V. Conclusions and Future Works

This paper discusses the challenges of autonomous vehicles due to occlusions that threaten their safety in urban scenarios. It presents a unified multi-occlusion aware model configuring phantom vehicles in the areas of interest where occlusions are complex. The proposed method employs the evidence theory to fuse measurements, enhancing occlusion inference. Simulations of an intersection scenario illustrated that the proposed method can generate more efficient trajectories for autonomous driving.

In the future, the model will be further improved by referencing other types of traffic participants. Moreover, the occlusion inference method will be extended to unstructured scenarios.

Acknowledgements

This work was supported in part by the Natural Science Foundation of China under Grant No. 61973239 and No. 62373284.

References

[1] R. Poncelet, A. Verroust-Blondet, and F. Nashashibi, "Safe geometric speed planning approach for autonomous driving through occluded intersections," in *the 16th International Conference on Control, Automation, Robotics and Vision (ICARCV)*. IEEE, 2020, pp. 393–399.

[2] S. K. Karanam, T. Duhautbout, R. Talj, V. Cherfaoui, F. Aioun, and F. Guillemard, "Virtual obstacle for a safe and comfortable approach to limited visibility situations in urban autonomous driving," in *Intelligent Vehicles Symposium (IV)*. IEEE, 2022, pp. 909–914.

[3] C. Hubmann, J. Schulz, M. Becker, D. Althoff, and C. Stiller, "Automated driving in uncertain environments: Planning with interaction and uncertain maneuver prediction," *IEEE Transactions on Intelligent Vehicles*, vol. 3, no. 1, pp. 5–17, 2018.

[4] C. Hubmann, N. Quetschlich, J. Schulz, J. Bernhard, D. Althoff, and C. Stiller, "A POMDP maneuver planner for occlusions in urban scenarios," in *Intelligent Vehicles Symposium (IV)*. IEEE, 2019, pp. 2172–2179.

[5] M.-Y. Yu, R. Vasudevan, and M. Johnson-Roberson, "Risk assessment

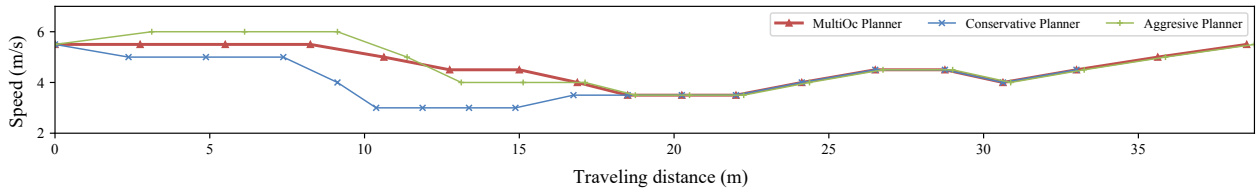

(a) Speed vs traveling distance

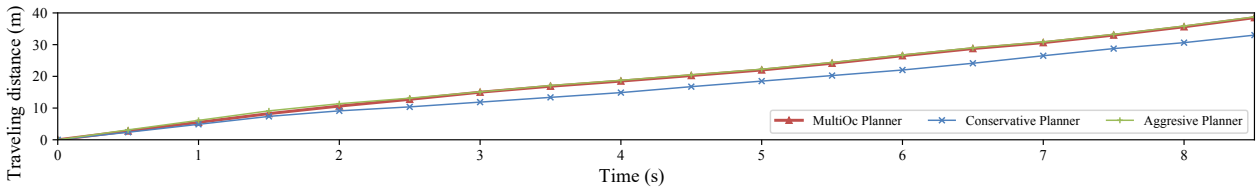

(b) Traveling distance vs time

Fig. 4: Planning results when the occluded area is free of vehicles.

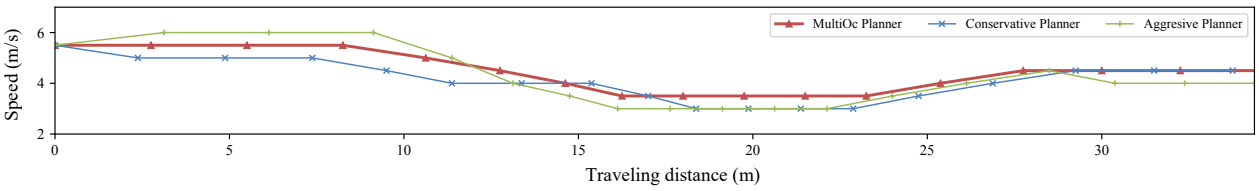

(a) Speed vs traveling distance

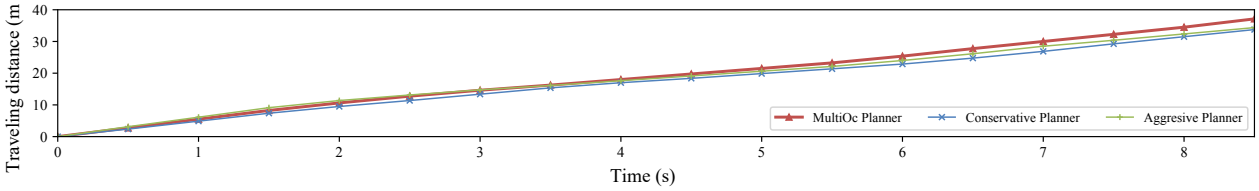

(b) Traveling distance vs time

Fig. 5: Planning results when the occluded area has an oncoming vehicle.

and planning with bidirectional reachability for autonomous driving," in *International Conference on Robotics and Automation (ICRA)*. IEEE, 2020, pp. 5363–5369.

[6] M. Koschi and M. Althoff, "Set-based prediction of traffic participants considering occlusions and traffic rules," *IEEE Transactions on Intelligent Vehicles*, vol. 6, no. 2, pp. 249–265, 2020.

[7] K. Hara, H. Kataoka, M. Inaba, K. Narioka, R. Hotta, and Y. Satoh, "Predicting appearance of vehicles from blind spots based on pedestrian behaviors at crossroads," *IEEE Transactions on Intelligent Transportation Systems*, vol. 23, no. 8, pp. 11 917–11 929, 2021.

[8] O. Afolabi, K. Driggs-Campbell, R. Dong, M. J. Kochenderfer, and S. S. Sastry, "People as sensors: Imputing maps from human actions," in *International Conference on Intelligent Robots and Systems (IROS)*. IEEE, 2018, pp. 2342–2348.

[9] M. Itkina, Y.-J. Mun, K. Driggs-Campbell, and M. J. Kochenderfer, "Multi-agent variational occlusion inference using people as sensors," in *International Conference on Robotics and Automation (ICRA)*. IEEE, 2022, pp. 4585–4591.

[10] L. Sun, W. Zhan, C.-Y. Chan, and M. Tomizuka, "Behavior planning of autonomous cars with social perception," in *Intelligent Vehicles Symposium (IV)*. IEEE, 2019, pp. 207–213.

[11] J. P. Hanna, A. Rahman, E. Fosong, F. Eiras, M. Dobre, J. Redford, S. Ramamoorthy, and S. V. Albrecht, "Interpretable goal recognition in the presence of occluded factors for autonomous vehicles," in *International Conference on Intelligent Robots and Systems (IROS)*. IEEE, 2021, pp. 7044–7051.

[12] P. Bender, J. Ziegler, and C. Stiller, "Lanelets: Efficient map representation for autonomous driving," in *Intelligent Vehicles Symposium Proceedings*. IEEE, 2014, pp. 420–425.

[13] M. Ramírez and H. Geffner, "Plan recognition as planning," in *Twenty-First International Joint Conference on artificial intelligence*, 2009.

[14] A. P. Dempster, "A generalization of bayesian inference," *Journal of the Royal Statistical Society: Series B (Methodological)*, vol. 30, no. 2, pp. 205–232, 1968.

[15] P. Smets, "Data fusion in the transferable belief model," in *Proceedings of the 3rd International Conference on Information Fusion*, vol. 1. IEEE, 2000, pp. PS21–PS33.

[16] K. J. Astrom *et al.*, "Optimal control of markov processes with incomplete state information," *Journal of mathematical analysis and applications*, vol. 10, no. 1, pp. 174–205, 1965.

[17] A. Somani, N. Ye, D. Hsu, and W. S. Lee, "Despot: Online POMDP planning with regularization," *Advances in Neural Information Processing Systems*, vol. 26, 2013.